INTERNATIONAL JOURNAL FOR NUMERICAL METHODS IN FLUIDS
Int. J. Numer. Meth. Fluids **29**: 737–748 (1999)

LATTICE BOLTZMANN SIMULATION OF FLOWS IN A THREE-DIMENSIONAL POROUS STRUCTURE

TAKAJI INAMURO*, MASATO YOSHINO AND FUMIMARU OGINO

Department of Chemical Engineering, Graduate School of Engineering, Kyoto University, Kyoto 606-8501, Japan

SUMMARY

The lattice Boltzmann method (LBM) with the fifteen-velocity model is applied to simulations of isothermal flows in a three-dimensional porous structure. A periodic boundary condition with a pressure difference at the inlet and outlet is presented. Flow characteristics at a pore scale and pressure drops through the porous structure are calculated for various Reynolds numbers. It is found that at high Reynolds numbers, unsteady vortices appear behind bodies and the flow field becomes time-dependent. Calculated pressure drops through the structure are compared with well-known empirical equations based on experimental data. The results agree well with the Blake–Kozeny equation for low Reynolds numbers and with the Ergun equation for high Reynolds numbers. Copyright © 1999 John Wiley & Sons, Ltd.

KEY WORDS: lattice Boltzmann method; periodic boundary condition; porous structure

1. INTRODUCTION

The problems of flows in porous media are very important in many science and engineering fields, such as geophysics, hydraulics, soil mechanics, chemical and petroleum engineering, and so on. In these problems, volume-averaged approaches are usually used to obtain macroscopic properties of flows in porous media. In order to estimate pressure drops in porous media the Blake–Kozeny equation [1] and the Ergun equation [2], which are both empirical equations based on experimental data, are often used for low and high Reynolds numbers respectively. In recent studies, Fand *et al.* [3] made experimental studies of flow through porous media composed of randomly packed spheres and proposed the useful correlation equations between pressure gradients and flow velocities. Liu *et al.* [4] studied laminar flows in porous media and presented a new averaging approach to the pressure gradient term. However, the relation between flow fields at a pore scale and pressure drops has not been so clear in these studies. In other words, the flow characteristics in porous media have not been investigated so clearly from the microscopic point of view.

As for numerical simulations, on the other hand, when conventional Navier–Stokes codes are applied to flows in porous media, one often has trouble with long computation times, poor convergence and numerical stabilities. Therefore, it is desired to develop another computational method. Rothman [5] and Chen *et al.* [6] used the lattice gas automata (LGA) for

* Correspondence to: Department of Chemical Engineering, Graduate School of Engineering, Kyoto University, Kyoto 606-8501, Japan.

CCC 0271–2091/99/070737–12$17.50

Received December 1997
Revised March 1998

simulations of flows through porous media to study microscopic behaviors occurring at a pore scale and to obtain volume-averaged parameters from the microscopic point of view. Succi *et al.* [7] and Cancelliere *et al.* [8] used the lattice Boltzmann method (LBM) [9,10] for similar problems. The main advantages of the LGA and LBM are the simplicity of the algorithm and the flexibility for complex geometries. However, the above mentioned simulations by the LGA and LBM were applied for relatively low Reynolds numbers and restricted in laminar flow regions. Recently, Inamuro *et al.* [11] have studied the problems of flow and heat transfer in a two-dimensional porous structure for a wide range of Reynolds numbers by using the LBM.

In the present paper, the LBM with the fifteen-velocity model [10] (a three-dimensional model) is used for simulations of flows in a three-dimensional porous structure for high Reynolds numbers as well as for low Reynolds numbers. Also, a periodic boundary condition with a pressure difference at the inlet and outlet is presented.

2. LATTICE BOLTZMANN METHOD

2.1. Method of computation

In the LBM, a modeled fluid, composed of identical particles whose velocities are restricted to a finite set of vectors $\mathbf{c}_i$, is considered and the evolution of particle population at each lattice site in physical space is computed. Hereafter, non-dimensional variables are used as in [12]. In the computation, the physical space is divided into a lattice, e.g. a cubic lattice for three-dimensional models. The evolution of the particle distribution function $f_i(\mathbf{x}, t)$ with velocity $\mathbf{c}_i$ at the point $\mathbf{x}$ and at time t is computed by the following equation [9,10]:

$$f_i(\mathbf{x}+\mathbf{c}_i\delta, t+\Delta t) - f_i(\mathbf{x}, t) = -\frac{1}{\tau}\rho(\mathbf{x}, t)[f_i(\mathbf{x}, t) - f_i^{\mathrm{eq}}(\mathbf{x}, t)], \tag{1}$$

where f_i^{eq} is an equilibrium distribution function, τ is a single relaxation time, δ is a lattice spacing, and Δt is a time step during which the particles travel the lattice spacing. The BGK model [13] is used for collision terms in Equation (1). As in the kinetic theory of gases, density ρ and flow velocity $\mathbf{u}$ are defined in terms of the particle distribution function as follows:

$$\rho = \sum_i f_i, \tag{2}$$

$$\mathbf{u} = \frac{1}{\rho}\sum_i f_i \mathbf{c}_i, \tag{3}$$

and pressure p is related to density ρ by [12]

$$p = \frac{1}{3}\rho. \tag{4}$$

It is found that using Equations (1)–(4), one can obtain the macroscopic flow velocities and the pressure gradient for incompressible fluid with relative errors of $O(\varepsilon'^2)$ where ε' is a modified Knudsen number that is of the same order as the lattice spacing δ and is related to the relaxation time τ [12].

2.2. Three-dimensional lattice model and equilibrium distribution function

The fifteen-velocity model [10], shown in Figure 1, is used for the following calculations. The velocity vectors of the particle of this model are given by

$$[\mathbf{c}_1, \mathbf{c}_2, \mathbf{c}_3, \mathbf{c}_4, \mathbf{c}_5, \mathbf{c}_6, \mathbf{c}_7, \mathbf{c}_8, \mathbf{c}_9, \mathbf{c}_{10}, \mathbf{c}_{11}, \mathbf{c}_{12}, \mathbf{c}_{13}, \mathbf{c}_{14}, \mathbf{c}_{15}]$$

$$= \begin{bmatrix} 0 & 1 & 0 & 0 & -1 & 0 & 0 & 1 & -1 & 1 & 1 & -1 & 1 & -1 & -1 \\ 0 & 0 & 1 & 0 & 0 & -1 & 0 & 1 & 1 & -1 & 1 & -1 & -1 & 1 & -1 \\ 0 & 0 & 0 & 1 & 0 & 0 & -1 & 1 & 1 & 1 & -1 & -1 & -1 & -1 & 1 \end{bmatrix}. \tag{5}$$

An equilibrium distribution function of this model is given by

$$f_i^{\mathrm{eq}} = E_i \rho \left[1 + 3\mathbf{c}_i \cdot \mathbf{u} + \frac{9}{2}(\mathbf{c}_i \cdot \mathbf{u})^2 - \frac{3}{2}\mathbf{u} \cdot \mathbf{u} \right] \quad \text{for} \quad i = 1, 2, 3, \ldots, 15, \tag{6}$$

where $E_1 = 2/9$, $E_2 = E_3 = E_4 = E_5 = E_6 = E_7 = 1/9$, and $E_8 = E_9 = E_{10} = E_{11} = E_{12} = E_{13} = E_{14} = E_{15} = 1/72$.

The viscosity μ of the fluid is related to the relaxation time τ and the lattice spacing δ by [12]

$$\mu = \frac{1}{3}\left(\tau - \frac{1}{2}\right)\delta. \tag{7}$$

3. BOUNDARY CONDITIONS

A three-dimensional porous structure shown in Figure 2 is considered. The structure consists of nine identical spherical bodies in a rectangular domain. A periodic boundary condition with a pressure difference is used at the inlet and outlet. The other faces are considered to be slip walls. Boundary conditions for particle distribution functions are needed in computations.

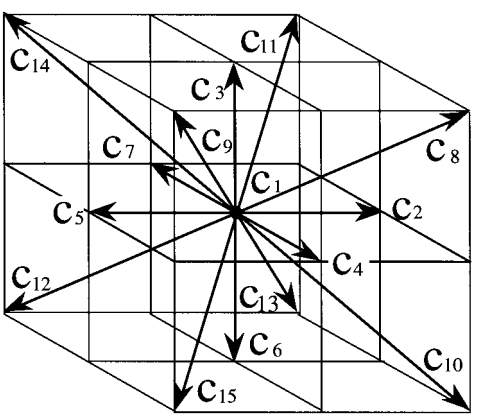

Figure 1. Fifteen-velocity model.

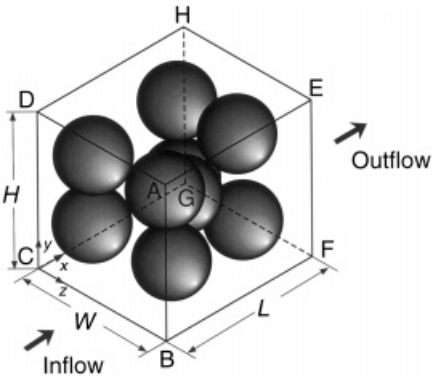

Figure 2. Three-dimensional porous structure.

3.1. At inlet and outlet

A periodic boundary condition with a pressure difference is used on the inlet at $x/L = 0$ and the outlet at $x/L = 1$ in Figure 2. Hereafter, the suffix 'in' and 'out' represent quantities at the inlet and outlet respectively. At the inlet and outlet, the unknown distribution functions, whose velocity points to the fluid region, are determined as follows. At the inlet, the unknown distribution functions are f_2, f_8, f_{10}, f_{11} and f_{13}. Taking account of the form of the equilibrium distribution functions given by Equation (6), and the fact that second- and higher-order terms of Knudsen number are regarded as errors [12], it is assumed that the unknown distribution functions at the inlet can be written by adding a constant value to the corresponding known distribution functions at the outlet as follows:

$$f_2|_{\text{in}} = f_2|_{\text{out}} + C, \tag{8}$$

$$f_i|_{\text{in}} = f_i|_{\text{out}} + \frac{1}{8} C \quad \text{for} \quad i = 8, 10, 11, 13. \tag{9}$$

Similarly, at the outlet the unknown distribution functions f_5, f_9, f_{12}, f_{14} and f_{15} are assumed to be written by subtracting a constant value from the corresponding known distribution functions at the inlet:

$$f_5|_{\text{out}} = f_5|_{\text{in}} - C, \tag{10}$$

$$f_i|_{\text{out}} = f_i|_{\text{in}} - \frac{1}{8} C \quad \text{for} \quad i = 9, 12, 14, 15. \tag{11}$$

Then the constant value C is determined so that the pressure difference between the inlet and outlet is equal to Δp. That is, using Equations (2) and (4), we get

$$C = \Delta p - \frac{1}{3}(f_1|_{\text{in}} - f_1|_{\text{out}} + f_3|_{\text{in}} - f_3|_{\text{out}} + f_4|_{\text{in}} - f_4|_{\text{out}} + f_6|_{\text{in}} - f_6|_{\text{out}} + f_7|_{\text{in}} - f_7|_{\text{out}}). \tag{12}$$

Substituting Equation (12) into Equations (8)–(11), all of the unknown distribution functions at the inlet and outlet are determined for the given Δp.

In addition, on the corner line, e.g. on the line BC, f_2, f_8, f_{10}, f_{11}, f_{13}, f_3, f_9 and f_{14} are unknown. In these unknown distribution functions, f_2, f_8, f_{10}, f_{11} and f_{13} are determined by the above mentioned procedure at the inlet, and the others f_3, f_9 and f_{14} are determined by the slip boundary condition described below.

3.2. On side of domain

As mentioned before, slip boundary conditions are assumed at the side wall. For example, at the lattice site on the face FBCG, f_3, f_8, f_9, f_{11} and f_{14} are unknown distribution functions and are simply determined as follows:

$$\left.\begin{aligned} f_3 &= f_6, \\ f_8 &= f_{10}, \\ f_9 &= f_{15}, \\ f_{11} &= f_{13}, \\ f_{14} &= f_{12}. \end{aligned}\right\} \tag{13}$$

On the corner line, e.g. on the line BF, f_3, f_8, f_9, f_{11}, f_{14}, f_7, f_{12} and f_{13} are unknown. In these unknowns, f_3, f_8, f_9, f_{11} and f_{14} are determined by Equation (13), and the others f_7, f_{12} and f_{13} are determined by regarding the line BF as a part of the face ABFE, i.e.

$$\left.\begin{aligned} f_7 &= f_4, \\ f_{12} &= f_{15}, \\ f_{13} &= f_{10}. \end{aligned}\right\} \tag{14}$$

Moreover, the unknown distribution functions at the vertex can be determined by the combination of the above mentioned conditions. For example, at the vertex B, the unknown distribution functions are f_2, f_3, f_7, f_8, f_9, f_{10}, f_{11}, f_{12}, f_{13} and f_{14}. In these unknown distribution functions, f_2, f_8, f_{10}, f_{11} and f_{13} are determined by the procedure at the inlet, and the others f_3, f_7, f_9, f_{12} and f_{14} are determined by the above mentioned slip boundary condition on the side.

3.3. At lattice site on body

In Figure 3, the lattice site P is a boundary point on the body and S is a tangential plane on the site P. $\mathbf{n}$ is the normal vector along the line connecting the site P with the center of the body. Then, two unit vectors perpendicular to $\mathbf{n}$ are defined as $\mathbf{t}$ and $\mathbf{b}$ so that $\mathbf{n}$, $\mathbf{t}$ and $\mathbf{b}$ are orthonormal bases. The velocity vectors of the particle are written in terms of the orthonormal bases as

$$\mathbf{c}_i = c_{in}\mathbf{n} + c_{it}\mathbf{t} + c_{ib}\mathbf{b}. \tag{15}$$

As seen from Figure 3, the distribution functions on the lattice site P such that $c_{in} > 0$ are unknown. The no-slip boundary condition [14] is applied to the present problem. Thus, the

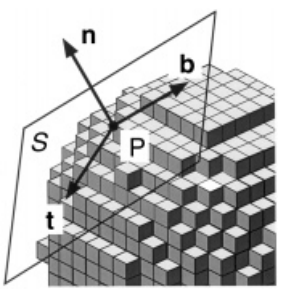

Figure 3. Tangential plane S on the lattice site of body and orthonormal bases $\mathbf{n}$, $\mathbf{t}$ and $\mathbf{b}$.

unknown distribution functions are assumed to be an equilibrium distribution function with a counter slip velocity, which is determined so that the fluid velocity at the surface is equal to zero. Then the unknown distribution functions are expressed by

$$f_i = E_i\rho'\left[1 + 3(c_{i\mathrm{t}}u'_{\mathrm{t}} + c_{i\mathrm{b}}u'_{\mathrm{b}}) + \frac{9}{2}(c_{i\mathrm{t}}u'_{\mathrm{t}} + c_{i\mathrm{b}}u'_{\mathrm{b}})^2 - \frac{3}{2}(u'^2_{\mathrm{t}} + u'^2_{\mathrm{b}})\right], \tag{16}$$

where ρ', u'_{t} and u'_{b} are unknown parameters. The unknown u'_{t} and u'_{b} are the counter slip velocity. The three unknown parameters are determined on the condition that the fluid velocity at the surface is zero. Thus, three equations corresponding to the three components of the fluid velocity are obtained. However, in the following, the counter slip velocities u'_{t} and u'_{b} are set to be zero, because the counter slip velocities often cause numerical instabilities for high Reynolds numbers. In the present calculations, therefore, the only unknown parameter ρ' is specified as follows:

$$\rho' = -\frac{\sum_{i(c_{i\mathrm{n}} \le 0)} c_{i\mathrm{n}} f_i}{\sum_{i(c_{i\mathrm{n}} > 0)} E_i c_{i\mathrm{n}}}. \tag{17}$$

4. RESULTS AND DISCUSSION

Flows in the three-dimensional porous structure, shown in Figure 2, are calculated. Nine identical bodies are included in the domain of $H = W = 0.945L$. The whole domain is divided into $73 \times 69 \times 69$ cubic lattice in the x-, y- and z-directions. The body is made up of a lattice block contained in a circumscribed sphere with a diameter of 28.4δ. It is expected that the equivalent diameter of the body D_{p} is larger than that of the circumscribed sphere, but one can not determine the value of D_{p} in advance of calculations. Here, we tried to determine the value of D_{p} by comparing a calculated pressure drop with the Blake–Kozeny equation at the lowest Reynolds number as explained below. The determined value of D_{p} is equal to 29.4δ. Then the porosity ε of the structure is 0.654. The centers of the bodies are located at $(x/L, y/H, z/W) =$ (0.21, 0.29, 0.22), (0.21, 0.74, 0.81), (0.22, 0.71, 0.22), (0.23, 0.32, 0.80), (0.48, 0.49, 0.49), (0.75, 0.80, 0.29), (0.78, 0.23, 0.70), (0.78, 0.78, 0.70) and (0.80, 0.23, 0.29). In the calculations, the pressure difference Δp between the inlet and outlet and the fluid viscosity μ are changed so that the range of the Reynolds numbers $Re = \bar{\rho}_{\mathrm{in}}\bar{u}_{\mathrm{in}}D_{\mathrm{p}}/\mu$ is $0.842 \le Re \le 159$, where $\bar{\rho}_{\mathrm{in}}$ $(= 1)$ and $\bar{u}_{\mathrm{in}}$ are the time- and space-averaged density and velocity at the inlet after transitional flows respectively. The initial conditions for the flow velocity and density are $\mathbf{u} = 0$ and $\rho = 1$ in the whole domain. In preliminary computations, also used were $38 \times 35 \times 35$ and $49 \times 46 \times 46$ cubic lattices. Then almost grid-independent results for low Reynolds numbers were obtained, but numerical instabilities for high Reynolds numbers occurred when the coarse grids were used.

Figures 4–6 show the calculated results of velocity vectors on the different planes ($y/H =$ 0.17, 0.62, and $x/L = 0.51$) for various Reynolds numbers after transitional flows. In these figures, the length of vectors is normalized so that the $\bar{u}_{\mathrm{in}}$ has the same length in spite of different Reynolds numbers, and the bodies in the structure are depicted by the spheres with the equivalent diameter D_{p}. It is found from Figures 4–6 that at low Reynolds number $Re = 0.842$, the fluid flow avoids the bodies and goes through open spaces. At $Re = 29.3$, on the other hand, the flow separations begin to occur and weak vortices appear behind the

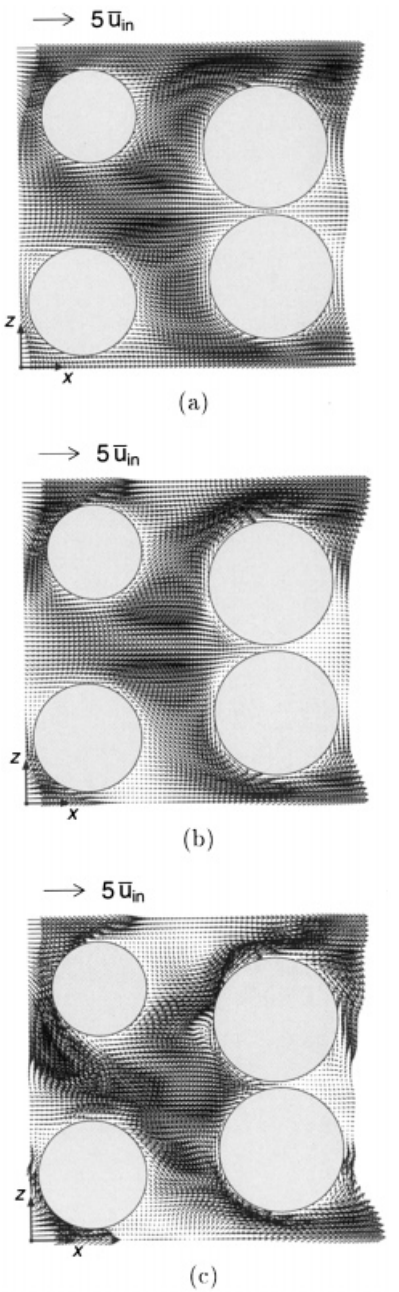

Figure 4. Velocity vectors on the plane $y/H = 0.17$ in the porous structure for various Reynolds numbers: (a) $Re = 0.842$, $\bar{u}_{in} = 4.29 \times 10^{-3}$; (b) $Re = 29.3$, $\bar{u}_{in} = 1.86 \times 10^{-2}$; (c) $Re = 159$, $\bar{u}_{in} = 4.37 \times 10^{-2}$.

bodies. At $Re = 159$, the vortices behind the bodies grow three-dimensionally and hence the flow field on $x/L = 0.51$ is quite different from those at the lower Reynolds numbers. Also, it is found that at the high Reynolds numbers, the strength of each vortex varies as time goes on, and the flow field becomes time-dependent.

Figure 7 shows the fluctuations of the x-component of the flow velocity u_x at the three different points in the domain for $Re = 159$. The three points are located at $(x/L, y/H, z/W) =$ (0.55, 0.17, 0.88), (0.45, 0.62, 0.09) and (0.51, 0.84, 0.14). It is found that large velocity fluctuations with a wide range of frequencies exist in the whole domain. In particular, the velocity

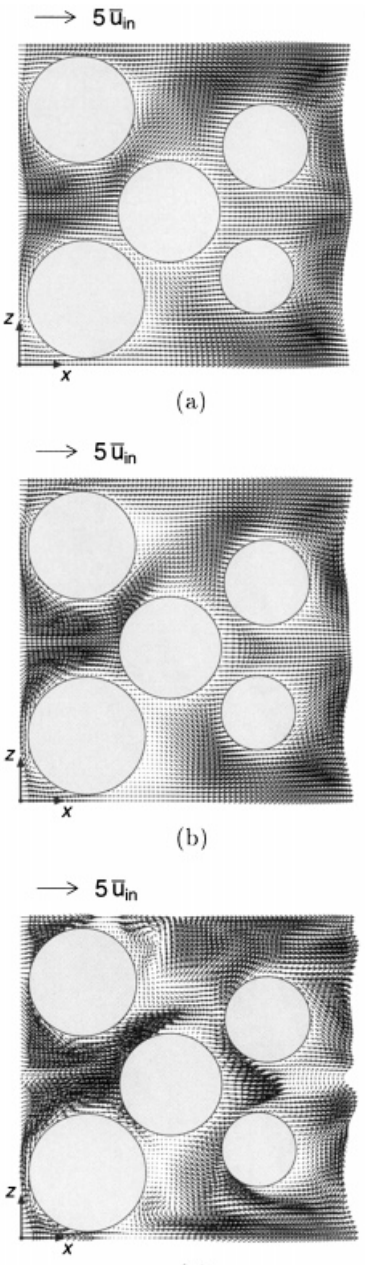

Figure 5. Velocity vectors on the plane $y/H = 0.62$ in the porous structure for various Reynolds numbers: (a) $Re = 0.842$, $\bar{u}_{in} = 4.29 \times 10^{-3}$; (b) $Re = 29.3$, $\bar{u}_{in} = 1.86 \times 10^{-2}$; (c) $Re = 159$, $\bar{u}_{in} = 4.37 \times 10^{-2}$.

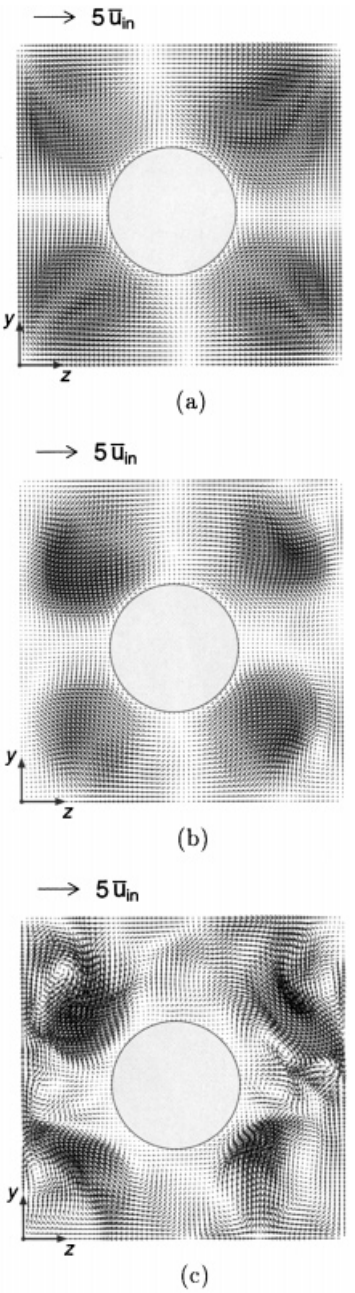

Figure 6. Velocity vectors on the plane $x/L = 0.51$ in the porous structure for various Reynolds numbers: (a) $Re = 0.842$, $\bar{u}_{in} = 4.29 \times 10^{-3}$; (b) $Re = 29.3$, $\bar{u}_{in} = 1.86 \times 10^{-2}$; (c) $Re = 159$, $\bar{u}_{in} = 4.37 \times 10^{-2}$.

fluctuation at $(x/L, y/H, z/W) = (0.51, 0.84, 0.14)$, where unsteady vortices exist as shown in Figure 6(c), has more high-frequency components than those at other points. Thus, it is seen that the flow field at $Re = 159$ becomes time-dependent and very complicated. In addition, it is noted that the time variation of the space-averaged velocity at the inlet in this case is only

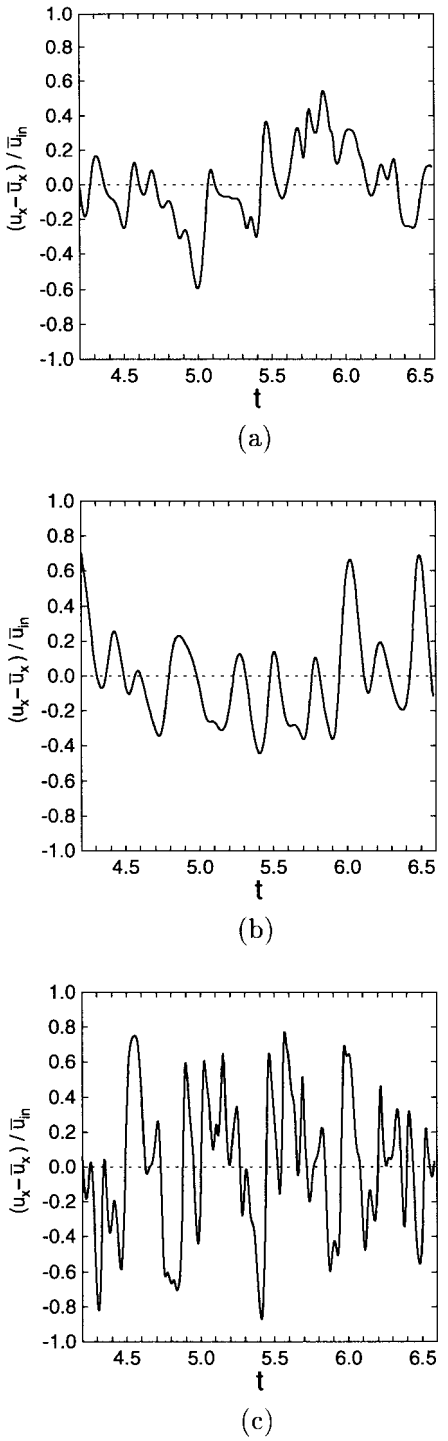

Figure 7. Fluctuations of the x-component of the flow velocity u_x at the three different points in the domain for $Re = 159$. The locations of the three points are (a) $(x/L, y/H, z/W) = (0.55, 0.17, 0.88)$; (b) $(x/L, y/H, z/W) = (0.45, 0.62, 0.09)$; (c) $(x/L, y/H, z/W) = (0.51, 0.84, 0.14)$. $\bar{u}_x$ is the time-averaged value of u_x. t is the dimensionless time based on the reference time t_0 during which the averaged inflow goes through the domain.

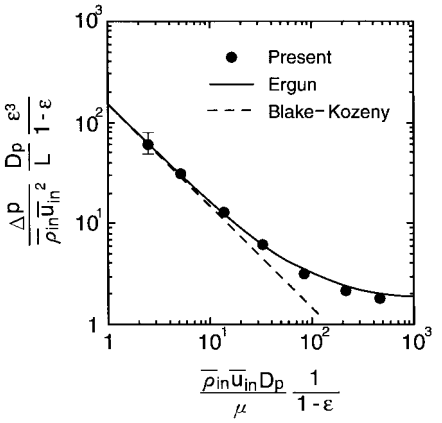

Figure 8. Pressure drop versus Reynolds numbers in the porous structure; ●, the present calculated results; – – –, the Blake–Kozeny equation [1]; —, the Ergun equation [2]. The error bar indicates the range of calculated results by changing D_p between 28.4δ and 30.4δ.

about 2% of the mean value in spite of the large time variations of the local velocity fields, as shown in Figure 7.

Finally, the calculated results of pressure drops are compared with empirical equations based on experimental data. Figure 8 shows the dimensionless pressure drops versus the Reynolds numbers multiplied by $1/(1-\varepsilon)$. It is noted that the porosity ε of the structure depends only on D_p when the whole rectangular domain is unchanged. As mentioned above, we tried to determine the value of D_p by comparing the calculated pressure drop with the Blake–Kozeny equation at the lowest Reynolds number. The error bar at the lowest Reynolds number in Figure 8 shows the range of the results calculated by changing the value of D_p between 28.4δ and 30.4δ. Comparing the calculated results with the Blake–Kozeny equation, it was found that a good agreement is obtained with $D_p = 29.4\delta$, as shown by the closed circle in Figure 8. Then, the same value of D_p was used for other Reynolds numbers. It is seen from Figure 8 that the calculated results of the pressure drops agree well with the empirical equations for the wide range of Reynolds numbers, although at high Reynolds numbers the calculated results become a little smaller than the Ergun equation. It is also found from Figures 4–6 and Figure 8 that the region of the Reynolds numbers where the pressure drops deviate from the Blake–Kozeny equation corresponds to the appearance of the vortices behind the bodies in the structure.

5. CONCLUDING REMARKS

The LBM with the fifteen-velocity model has been applied to simulations of flows in a three-dimensional porous structure. Flow fields at a pore scale and pressure drops through the structure are obtained for various Reynolds numbers. The calculated pressure drops agree well with the empirical equations based on experimental data. Consequently, it was found that the LBM is useful for the investigation of microscopic properties of flows in porous media. It is also noted that one can apply the LBM to the problems of heat and mass transfer using other velocity models for heat-conducting and multicomponent fluids.

ACKNOWLEDGMENTS

This research was partly supported by the Grant-in-Aid (No. 07650894) for Scientific Research from the Ministry of Education, Science and Culture in Japan and the General Sekiyu R&D Encouragement and Assistance Foundation.

REFERENCES

1. R.B. Bird, W.E. Stewart and E.N. Lightfoot, *Transport Phenomena*, Wiley, New York, 1960, p. 199.
2. S. Ergun, 'Fluid flow through packed columns', *Chem. Eng. Prog.*, **48**, 89–94 (1952).
3. R.M. Fand, B.Y.K. Kim, A.C.C. Lam and R.T. Phan, 'Resistance to the flow of fluids through simple and complex porous media whose matrices are composed of randomly packed spheres', *Trans. ASME*, **109**, 268–274 (1987).
4. S. Liu, A. Afacan and J. Masliyah, 'Steady incompressible laminar flow in porous media', *Chem. Eng. Sci.*, **49**, 3565–3586 (1994).
5. D.H. Rothman, 'Cellular-automaton fluids: a model for flow in porous media', *Geophysics*, **54**, 509–518 (1988).
6. S. Chen, K. Diemer, G.D. Doolen, K. Eggert, C. Fu, S. Gutman and B.J. Travis, 'Lattice gas automata for flow through porous media', *Physica D*, **47**, 72–84 (1991).
7. S. Succi, E. Foti and F. Higuera, 'Three-dimensional flows in complex geometries with the lattice Boltzmann method', *Europhys. Lett.*, **10**, 433–438 (1989).
8. A. Cancelliere, C. Chang, E. Foti, D.H. Rothman and S. Succi, 'The permeability of a random medium: comparison of simulation with theory', *Phys. Fluids A*, **2**, 2085–2088 (1990).
9. G. McNamara and G. Zanetti, 'Use of the Boltzmann equation to simulate lattice-gas automata', *Phys. Rev. Lett.*, **61**, 2332–2335 (1988).
10. Y.H. Qian, D. d'Humières and P. Lallemand, 'Lattice BGK models for Navier–Stokes equation', *Europhys. Lett.*, **17**, 479–484 (1992).
11. T. Inamuro, M. Yamamura and F. Ogino, 'Lattice Boltzmann simulation of flow and heat transfer in a two-dimensional porous structure', in C. Taylor and P. Durbetaki (eds.), *Numerical Methods in Laminar and Turbulent Flow*, vol. 9, Pineridge Press, Swansea, 1995, pp. 632–643.
12. T. Inamuro, M. Yoshino and F. Ogino, 'Accuracy of the lattice Boltzmann method for small Knudsen number with finite Reynolds number', *Phys. Fluids*, **9**, 3535–3542 (1997).
13. P.L. Bhatnagar, E.P. Gross and M. Krook, 'A model for collision processes in gases. I. Small amplitude processes in charged and neutral one-component systems', *Phys. Rev.*, **94**, 511–525 (1954).
14. T. Inamuro, M. Yoshino and F. Ogino, 'A non-slip boundary condition for the lattice Boltzmann simulations', *Phys. Fluids*, **7**, 2928–2930; Erratum: *Phys. Fluids*, **8**, 1124 (1996).

